NUMERICAL ANALYSES OF A HYDRAULIC HYBRID POWERTRAIN SYSTEM FOR A TRANSIT BUS

Marko N. KITANOVIĆ*[*1], Slobodan J. POPOVIĆ[1], Nenad L. MILJIĆ[1], Predrag D. MRĐA[1]

[1]University of Belgrade, Faculty of Mechanical Engineering, Belgrade, RS

[*] Corresponding author; E-mail: mkitanovic@mas.bg.ac.rs

A Dynamic Programming (DP) optimization algorithm has been applied on a transit bus model in MATLAB in order to assess the fuel economy improvement potential by implementing a hydraulic hybrid powertrain system. The numerical model parameters have been calibrated using experimental data obtained on a Belgrade's public transport bus. This experiment also provided the representative driving cycle on which to conduct simulation analyses. Various functional parameters of a hydraulic hybrid system have been evaluated for obtaining the best possible fuel economy. DP optimization runs have been completed for various hydraulic accumulator sizes, preload values and accumulator foam quantities. It has been shown that a fuel economy improvement of 28% can be achieved by implementing such a system.

Key words*: hydraulic hybrid, internal combustion engines, transit bus, optimization, dynamic programming*

1. Introduction

An ever-increasing amount of effort in the research community is being invested in alternative powertrain systems, with the goal of improving the vehicle fuel economy by utilizing the energy normally wasted during the braking phases. A considerable number of studies have been published that deal with fuel economy improvements and implementation aspects of alternative powertrain systems on transit buses, such as hybrid electric solutions using batteries and/or ultracapacitors for regenerative energy storage, or hydraulic hybrid solutions [1, 2 and 3].

The intention of the research that is presented in this paper has been to assess the potential for fuel economy improvement of a hydraulic hybrid powertrain system implemented on a transit bus vehicle. Previously, similar studies have been carried out in [4, 5], dealing with energetic and simulation studies of hybrid electric systems. The characteristics of hydraulic hybrid systems make it an interesting alternative to other hybrid configurations due to the high specific power of the pump/motor and hydro-pneumatic accumulator. On the other hand, the specific energy of the hydro-pneumatic accumulator is considerably less than that of electrochemical batteries, which renders its use problematic with regards to the optimal control law that shall make the most of its limited capacity [6].

In the next chapter, the methodology used to perform the simulation study is presented, along with the models of the vehicle and hydraulic components. Then, simulation results are given in a subsequent chapter, and, finally, conclusions are laid out.

2. Methodology of the simulation experiment

In order to be able to conduct numerical analyses of alternative powertrain systems and determine the configuration that would bring the most benefits with regard to fuel economy improvements, having a calibrated conventional transit bus powertrain system model is essential. This is the reason a comprehensive data-acquiring experiment has been performed on a public transport service bus in Belgrade [4, 5]. This endeavor has allowed the calibration of a MATLAB model of a conventional transit bus powertrain that has served afterwards as an input for DP optimization runs involving various hydraulic hybrid configurations. Rolling friction coefficients, aerodynamic friction coefficients, the engine BSFC and brake torque limits maps, along with data concerning the gearbox, hydrodynamic torque converter and various drivetrain components among others, have been implemented into the base model. Detailed procedures and values can be found in [4, 5 and 7].

Driving cycles have also been extracted from this acquired data. It should be mentioned that they have been obtained in real traffic and occupancy conditions, allowing numerical analyses to be performed for different representative conditions. A driving cycle with moderate traffic congestion has been used in this study. Its velocity and elevation/road slope profiles are shown in Fig. 1 and Fig. 2.

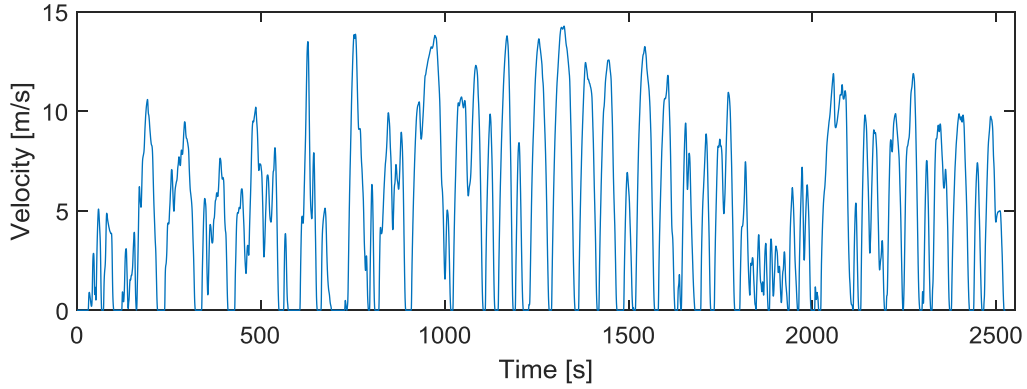

Fig. 1 Vehicle velocity profile

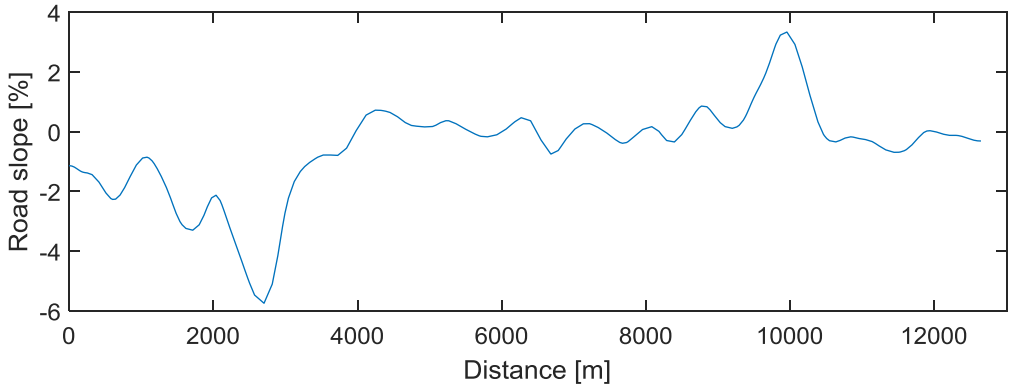

Fig. 2 Road slope profile

2.1. Hydraulic hybrid powertrain system components

In this section of the article, a short review of the mathematical models for the hydraulic system components is given.

2.1.1 Hydraulic pump/motor

A 250 cm^3, variable displacement swashplate axial piston pump (Rexroth A4VSO) has been used as the main hydraulic unit for recuperating the regenerative braking energy and subsequently providing traction to the vehicle during acceleration phases. A fixed ratio (1.2) gearbox is positioned between the pump and the vehicle drivetrain in order to match the operational range of the hydraulic unit with the engine speed range. A drive power and flow map is given in Fig. 3.

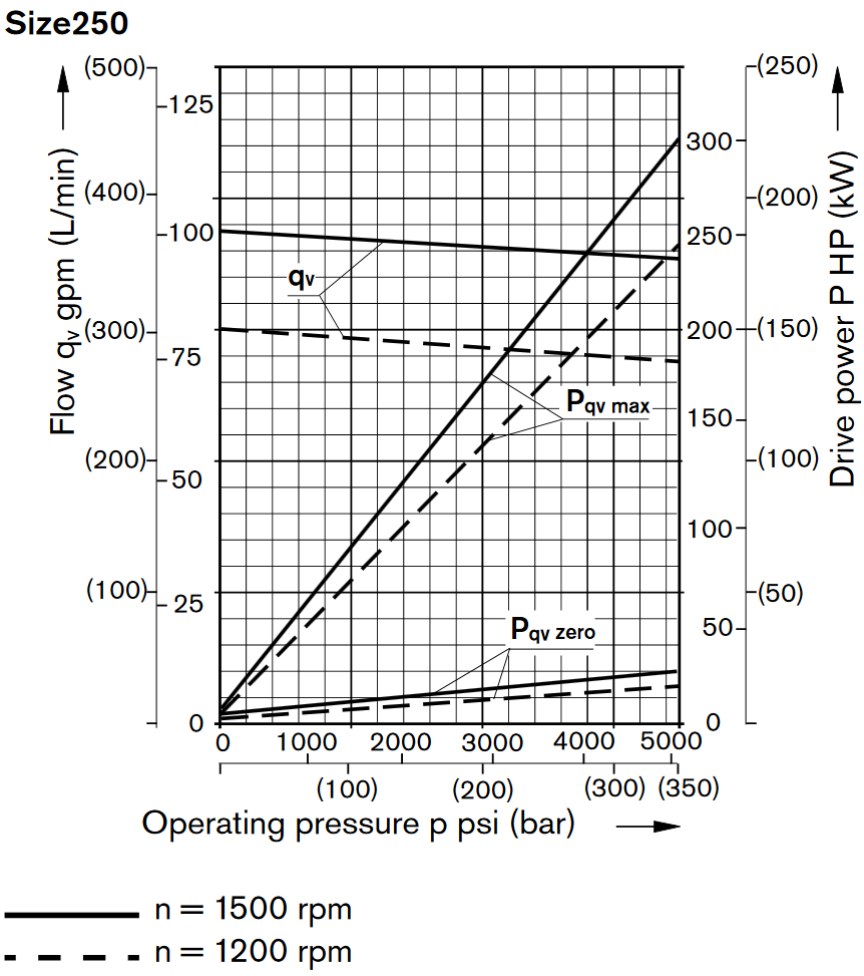

Fig. 3 Hydraulic pump drive power and flow characteristics [8]

Using the given pump characteristics data, a complete operating map had to be derived in order to conduct the simulation and control optimization routines. A hydraulic pump/motor model from [9] has been utilized for that purpose. The ideal volumetric flow rate through a pump or motor is given by

$$Q_i = x\omega D, \tag{1}$$

where x is the ratio of actual and maximum unit capacity, ω is the pump/motor angular speed and D is the maximum pump/motor displacement per radian.

The pump volumetric efficiency is the ratio of the actual to the ideal flow rate:

$$\eta_{v,p} = \frac{Q_a}{Q_i}. \tag{2}$$

For the motor mode, the volumetric efficiency is the inverse of the previous expression:

$$\eta_{v.m} = \frac{Q_i}{Q_a}. \tag{3}$$

On the other hand, these coefficients can be expressed using laminar and turbulent leakage coefficients, among others:

$$\eta_{v,p} = 1 - \frac{C_s}{xS} - \frac{\Delta p}{\beta} - \frac{C_{st}}{x\sigma}, \tag{4}$$

where C_s and C_{st} are the laminar and turbulent leakage coefficients, respectively and β is the bulk modulus of elasticity of the oil. The dimensionless numbers S and σ are defined as:

$$S = \frac{\mu\omega}{\Delta p}, \tag{5}$$

$$\sigma = \frac{\omega D^{1/3}}{\left(2\frac{\Delta p}{\rho}\right)^{1/2}}. \tag{6}$$

For the hydraulic motor, we can express the volumetric efficiency as

$$\eta_{v,m} = \frac{1}{1 + \frac{C_s}{xS} + \frac{\Delta p}{\beta} + \frac{C_{st}}{x\sigma}}. \tag{7}$$

The torque required to operate an ideal pump is given by

$$T_i = x \cdot \Delta p \cdot D. \tag{8}$$

The pump mechanical efficiency is defined by the following ratio:

$$\eta_{t,p} = \frac{T_i}{T_a}, \tag{9}$$

where T_a is the actual torque. The motor mechanical efficiency is defined by

$$\eta_{t,m} = \frac{T_a}{T_i}. \tag{10}$$

The pump torque efficiency can be expressed with the following expression:

$$\eta_{t,p} = \frac{1}{1 + \frac{C_v S}{x} + \frac{C_f}{x} + C_h x^2 \sigma^2}, \tag{11}$$

whereas the motor torque efficiency is defined as:

$$\eta_{t,m} = 1 - \frac{C_v S}{x} - \frac{C_f}{x} - C_h x^2 \sigma^2. \tag{12}$$

C_v, C_f and C_h are the viscous, frictional and the hydrodynamic loss coefficients, respectively.

By using the previously described model and the available data, the volumetric efficiency leakage coefficients (laminar and turbulent) and the mechanical efficiency coefficients (viscous, frictional and hydrodynamic loss coefficients) have been calculated and thus a full pump/motor map has been formed.

2.1.2 Hydro-pneumatic accumulator

The hydro-pneumatic accumulator gathers energy during the vehicle deceleration phases by means of the hydraulic fluid entering its chamber and compressing the nitrogen gas stored inside a compressible bladder. This energy is then used to propel the vehicle in subsequent acceleration phases, which depletes the hydro-pneumatic accumulator of its oil and readies it for energy accumulation again. A significant fraction of the input energy (on the order of several tens of percent) can be lost to thermal transfer to the accumulator wall and its surroundings. This loss can be diminished by inserting an elastomeric foam with a very high surface area and specific heat into the accumulator. In this way, temperature variations caused by gas compressions and expansions are appreciably reduced and only a fraction of the original energy loss occurs.

Compared to electrical batteries, hydro-pneumatic accumulators are characterized by a higher specific power and a lower specific energy. Its high specific power renders it suitable for heavy vehicles with frequent acceleration/deceleration phases. On the other hand, the low specific energy represents a disadvantage due to the limited braking recuperation potential and is a challenge that must be overcome in order to maximize the fuel economy benefits of the hydraulic hybrid system.

In this study, a two state simulation model of a hydro-pneumatic accumulator has been used. The first state variable - gas temperature T is derived from the gas energy equation [9]:

$$\left(\tau + \frac{m_f c_f}{h A_w}\right)\frac{dT}{dt} + T = T_w - \frac{T\tau}{c_v}\left(\frac{\partial p_g}{\partial T}\right)_v \frac{dv}{dt}, \tag{13}$$

where

$$\tau = \frac{m_g c_v}{h A_w} \tag{14}$$

is the thermal time constant. Due to high pressures encountered in the accumulator, the ideal gas law cannot be used with sufficient accuracy. Instead, a Benedict-Webb-Rubin equation of state has been used for modeling the state of the nitrogen gas:

$$p_g = \frac{RT}{v} + \frac{1}{v^2}\left(B_0 RT - A_0 - \frac{C_0}{T^2}\right) + \frac{bRT - a}{v^3} + \frac{a\alpha}{v^6} + \frac{c}{v^3 T^2}\left(1 + \frac{\gamma}{v^2}\right)\exp^{-\gamma/v^2}, \tag{15}$$

where the corresponding coefficients for nitrogen are taken from [10]. By combining Eqs. 13 and 15, we can obtain the following expression:

$$\left(1 + \frac{m_f c_f}{m_g c_v}\right)\frac{dT}{dt} = \frac{T_w - T}{\tau} - \frac{1}{c_v}\left\{\frac{RT}{v}\left(1 + \frac{b}{v^2}\right) + \frac{1}{v^2}\left(B_0 RT + \frac{2C_0}{T^2}\right) - \frac{2c}{v^3 T^2}\left(1 + \frac{\gamma}{v^2}\right)\exp^{-\gamma/v^2}\right\}\frac{dv}{dt}. \tag{16}$$

The second state variable, specific volume v, is derived from the continuity equation

$$\frac{dv}{dt} = \frac{Q_a}{m_g}, \tag{17}$$

where Q_a is the pump/motor actual flow rate and m_g is the accumulator gas mass.

For evaluating the accumulator states during DP runs, the previous equations have been discretized and brought to a form suitable for the Runge-Kutta method.

2.2. Dynamic programming

Dynamic programming is a technique for solving optimal control problems. It has been used in this study to derive the optimal load distribution between the hydraulic pump/motor and the internal combustion engine, subject to various constraints and conditions, in order to minimize the fuel consumption. This method can be used for different hybrid powertrain designs and component sizes, allowing us to assess the maximal fuel economy improvement potential for a given hybrid configuration and a vehicle/driving cycle combination.

Dynamic programming relies on the principle of optimality, which states that [11] "An optimal policy has the property that whatever the initial state and initial decision are, the remaining decisions must constitute an optimal policy with regard to the state resulting from the first decision."

By decomposing a control problem into segments or sub-problems, an optimal decision can be discovered at each stage, starting from the end and moving toward the initial instant. By defining the allowable final system state constraints, a dynamic programming algorithm starts with evaluating the

optimal decision at the stage preceding the final stage that will result in the system reaching this final state at minimal cost. This is done by discretizing the state space, which results in a time-state space grid with nodes at which the cost is evaluated by sweeping the admissible control values, subject to state constraints. By proceeding backwards, an optimal control decision can be stated for each stage-state combination that will bring the system from the current stage-state point to the desired final state at minimal cost. By ultimately reaching the initial time stage, the cost-to-go and optimal control matrices are obtained, representing respectively the cost and optimal control decisions for each admissible stage-state combination. Mathematically, this can be stated through a recurrence relation [12]:

$$J^*_{N-K,N}\left(\vec{x}\left(N-K\right)\right)=\min_{u(N-K)}\left\{\begin{matrix} g_D\left(\vec{x}\left(N-K\right),\vec{u}\left(N-K\right)\right)+ \\ +J^*_{N-(K-1),N}\left(\vec{a}_D\left(\vec{x}\left(N-K\right),\vec{u}\left(N-K\right)\right)\right)\end{matrix}\right\}. \quad (18)$$

By knowing $J^*_{N-(K-1),N}$, the optimal cost at the (K-1) stage, the optimal cost for the K stage $J^*_{N-K,N}$ can be determined, along with its corresponding control.

Only one control variable is used in the DP algorithm in this study. In traction phases, this control variable represents the engine to hydraulic motor torque ratio. In braking phases, its definition shifts to being the ratio of hydraulic pump and friction brakes torque values.

A generic MATLAB implementation of the dynamic programming algorithm has been used in this study [13].

2.3. Design parameters variation

Several design parameters concerning the hydro-pneumatic accumulator have been varied in this simulation study in order to analyze the impact of these variables on fuel economy. Hydro-pneumatic accumulator preload is one of them. It is defined as the pressure of the gas when the accumulator is completely depleted (of hydraulic oil), at a predetermined temperature, meaning that it is correlated to a given nitrogen gas mass inside the accumulator. The accumulator capacity (volume) and the elastomeric foam mass variations are included. A summary of the values assumed for the design parameters is given in Table 1.

Table 1 – Hydro-pneumatic design parameters variation values

Design parameter	Name	Unit	Case 1	Case 2
Preload	‘preload’	[bar]	70, 90, 110, 130, 150	70, 90, 110, 130, 150
Volume	‘accu’	[dm^3]	50	30, 50, 70, 90
Foam mass	‘mf’	[kg]	0, 3, 6	=1.233·mg
Gas mass	‘mg’	[kg]	=f(preload)	=f(preload,accu)
Thermal time constant	‘tau’	[s]	=f(mg)	=f(mg,accu)

In case 1, the independent variables are the hydro-pneumatic accumulator preload and the foam mass. The accumulator gas mass is calculated based on the accumulator volume, the preload pressure, the reference temperature (320 [K]) and the real gas factor *Z*. The reference accumulator thermal time constant is modified to take into account the different nitrogen gas mass values at the predetermined

preload setpoints. In case 2, the goal has been to assess the optimal hydro-pneumatic accumulator volume and its corresponding optimal preload value for the given hydraulic hybrid powertrain system and the considered driving cycle. The foam mass has been held at a fixed ratio (1.233) of the accumulator nitrogen gas mass. For the accumulator gas mass, apart from its dependency on the preload pressure, the influence of the accumulator volume has also been introduced in this case. Similarly, the accumulator thermal time constant dependency on the accumulator capacity by means of the total wall area had to be taken into account due to the accumulator volume being an independent variable in the mentioned case.

It should be noted that the specific heat of the accumulator foam is fixed at 2300 [$Jkg^{-1}K^{-1}$], while a temperature-dependency specific heat model (NASA Glenn Coefficients [14]) is used for the nitrogen gas.

With regard to the constraints set in the analyses, the allowable nitrogen gas temperature range is from 280 [K] to 400 [K] and the maximum allowed accumulator pressure is set to 350 [bar]. The maximum specific volume of the nitrogen gas is calculated using the Benedict-Webb-Rubin equation of state using the total accumulator volume and the reference temperature. The minimum specific volume is set to a value corresponding to the volume of the gas at the maximum pressure and minimum temperature. The hydro-pneumatic accumulator wall temperature is set to a constant value of 320 [K].

3. Results

In this section of the article, results of the DP simulation runs are shown and discussed.

3.1. Case 1

The results of the case 1, where the independent variables are the hydro-pneumatic accumulator preload and the foam mass, will be analyzed next.

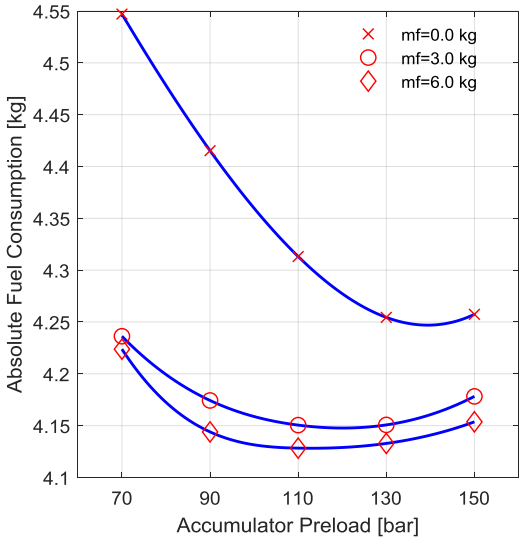

Fig. 4 Absolute fuel consumption for case 1

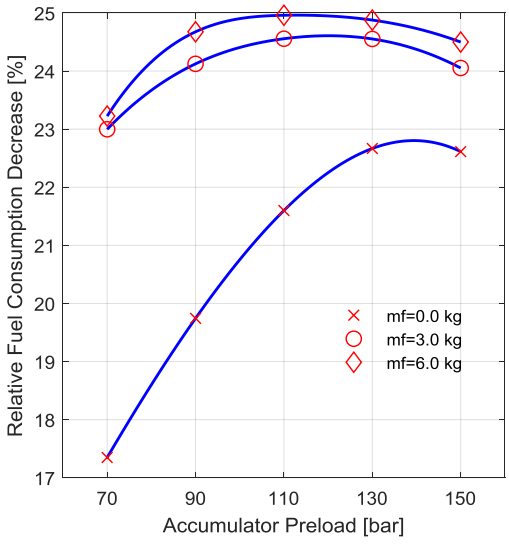

Fig. 5 Relative fuel consumption decrease for case 1

The Fig. 4 shows the absolute quantity of fuel consumed for the given driving cycle, whereas Fig. 5 shows the relative fuel consumption decrease compared to the conventional transit bus

powertrain. It is evident that the impact of the elastomeric foam on the performance of the accumulator is considerable. For the foam-less accumulator, a drastic reduction in fuel economy improvement occurs at lower preload pressure values. Namely, by adding 6 [kg] of foam mass to a foam-less accumulator at the preload pressure of 70 [bar], an additional fuel economy improvement in excess of 6% can be achieved. The marginal fuel economy improvement between the hydro-pneumatic accumulator with 3 [kg] and 6 [kg] of elastomeric foam is approximately 0.5%.

Figure 6 shows what would happen to the pressure and temperature traces of the nitrogen gas inside the hydro-pneumatic accumulator for different quantities of the elastomeric foam mass and for a given section of the driving cycle. It is evident that the foam-less accumulator achieves lower pressures following a regenerative braking event. This can be explained by analyzing the temperature traces of the braking event. It can be seen that what limits the pressure rises is the constraint placed on the maximum nitrogen temperature. By increasing the foam mass for a given nitrogen gas mass, the temperature variations inside the accumulator are diminished and the constraints are reached later, if hit at all, allowing more energy to be harnessed and greater gas pressures to be achieved.

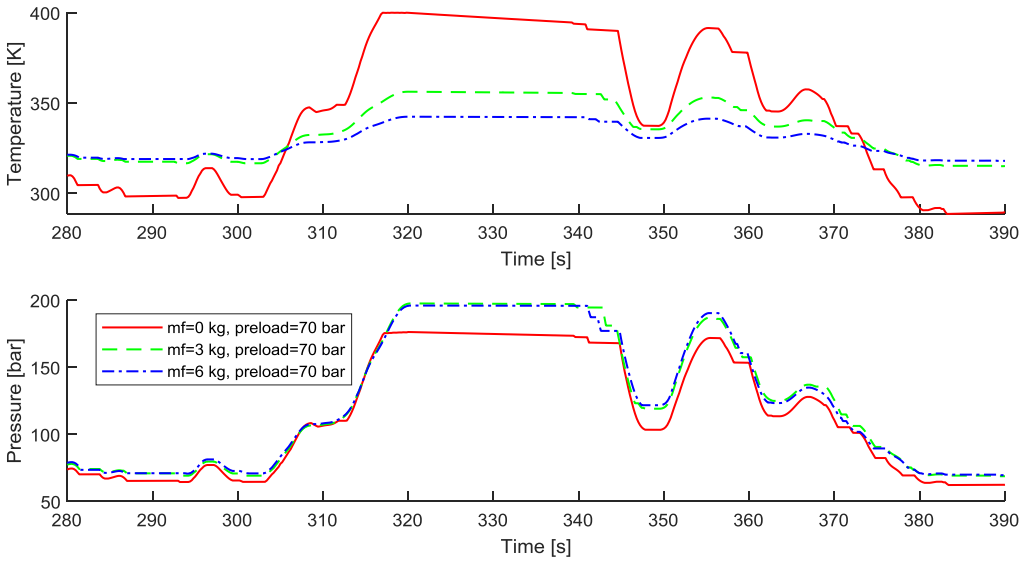

Fig. 6 Hydro-pneumatic accumulator pressure and temperature traces dependency on the foam mass for a section of the driving cycle in case 1

What can also be observed in case 1 is the influence of the foam mass on the optimal preload pressure. Namely, the optimal preload pressure decreases with rising elastomeric foam mass. By increasing the preload accumulator pressure, a higher mean pressure can be expected (Fig. 7), causing a rise in the potential torque available at the hydraulic pump/motor unit. A higher preload pressure also means higher nitrogen gas mass, which for a given hydraulic accumulator wall surface area raises the thermal time constant. On the other hand, for a given foam mass inside the accumulator, decreasing the preload pressure causes the foam/gas mass ratio to increase, which diminishes the temperature variations and thus potentially allows more energy flow for the given temperature constraints.

Figure 8 shows the round-trip efficiency of the hydraulic hybrid powertrain for case 1. It is calculated by dividing the mechanical energy delivered from the hydraulic motor to the powertrain

with the energy absorbed by the pump. Even though maximal values of the hybrid system efficiency of approximately 77% are achieved at the lowest accumulator preload settings, the optimal fuel efficiencies are obtained at higher preload values of 110 to 130 [bar] for the accumulators with elastomeric foam mass. This is caused by the correspondingly greater levels of mechanical energy absorbed at those increased preload values. The principal influence on the declining trend of this round-trip efficiency with increasing preload values is the volumetric efficiency, which decreases with rising accumulator pressures. The lower efficiencies for the foam-less accumulator can be explained by the lower hydraulic pump/motor loads during the driving cycle.

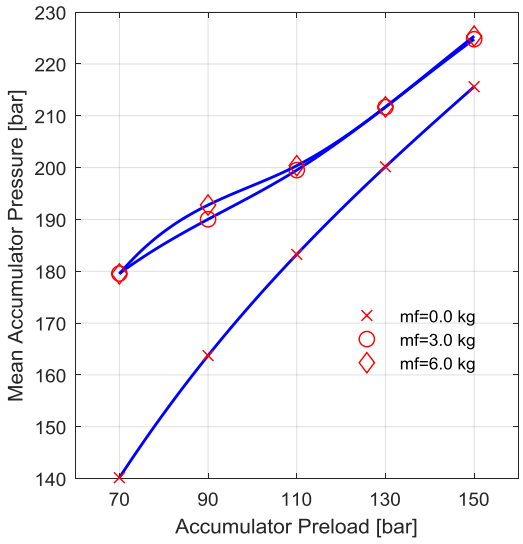

Fig. 7 Mean accumulator gas pressure for case 1

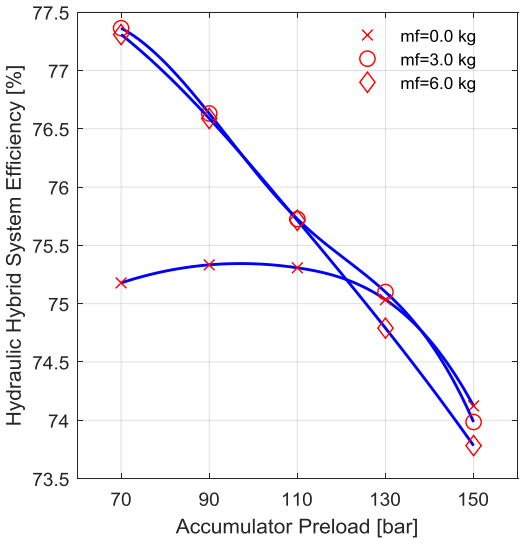

Fig. 8 Round-trip efficiency for case 1

3.2. Case 2

As outlined earlier, in case 2, two independent variables have been introduced: the accumulator volume and preload pressure. What follows is the analysis of the results.

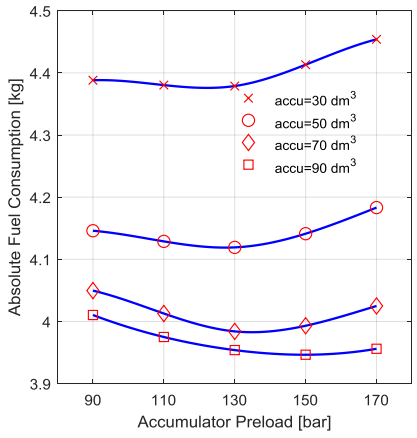

Fig. 9 Absolute fuel consumption for case 2

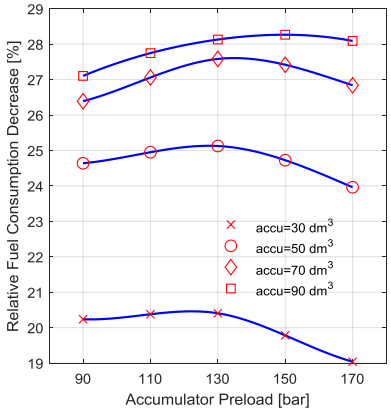

Fig. 10 Relative fuel consumption decrease for case 2

Because a proportional dependency of the accumulator volume on the total wall area was assumed, the resulting thermal time constant values effectively change (rising) only with the preload pressure.

Figures 9 and 10 show that the maximal fuel economy improvement of 28.3% is obtained with the largest accumulator of 90 [l]. The best fuel economy improvement potential of the smallest accumulator is 20.4%. It should be noted that the marginal improvement in fuel consumption diminishes after 50 [l]. Namely, increasing the accumulator capacity from 70 to 90 [l] brings only an additional improvement of approximately 0.7% in fuel economy.

By increasing the accumulator volume, the masses of the nitrogen gas and the elastomeric foam increase, reducing the temperature variations of the gas inside the hydro-pneumatic accumulator. This has a beneficial effect on the efficiency of the accumulator. On the other hand, increasing the accumulator capacity reduces the mean nitrogen gas pressure during the driving cycle (Fig. 11), reducing the potential torque available at the hydraulic pump/motor unit. However, this disadvantage is offset by a correspondingly greater energy accumulation potential, bringing a net improvement in fuel economy. It is also noticeable that the optimal preload pressure values increase with rising accumulator capacities.

Figure 12 shows the round-trip efficiency of the hydraulic hybrid powertrain achieved during the DP runs for case 2. It can be concluded that the accumulator capacity has a negligible influence on the hybrid system efficiency, with the maximal difference reaching values just over 1%. The influence of the preload pressure on the round-trip efficiency shows a trend comparable to the results in case 1. Namely, the efficiency decreases with rising preload pressure values, which can be explained by the declining volumetric efficiency of the hydraulic unit.

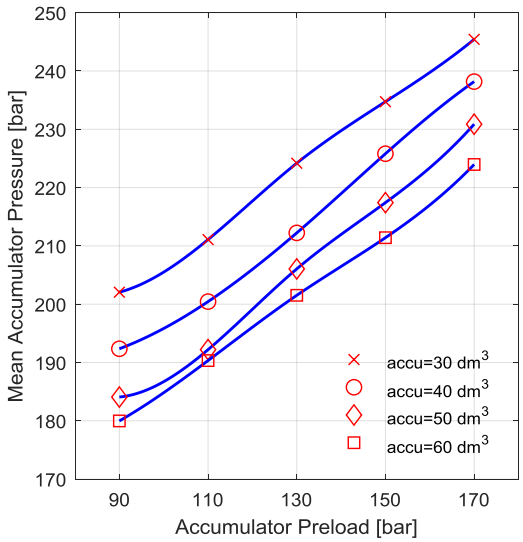

Fig. 11 Mean accumulator gas pressure for case 2

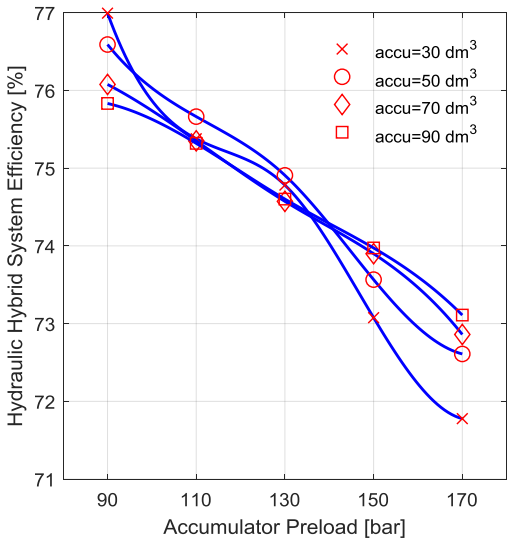

Fig. 12 Round-trip efficiency for case 2

4. Concluding remarks

A dynamic programming simulation model has been designed in order to assess the maximal fuel economy improvement potential of a parallel hydraulic hybrid powertrain system. Several

analyses have been performed in order to quantify the influence of key hydro-pneumatic accumulator design parameters on the hybrid powertrain fuel economy figures. It has been found that significant fuel consumption improvements in the range of 20% to 28% can be achieved by implementing such a system.

Additional efforts should be concentrated on further simulation analyses with the goal of optimizing the energy accumulation potential of the hydraulic hybrid system. Although dynamic programming has proved helpful in quantifying the influences of several design parameters on the fuel economy, a review of the implementable control algorithms should also be conducted in order to assess the best possible solution that can be used on the vehicle.

Acknowledgment

The research presented in this paper is conducted in the framework of the research project TR35042, titled "Research and Development of Alternative Fuel and Drive Systems for Urban Buses and Refuse Vehicles with Regard to the Improvements of Energy Efficiency and Environmental Characteristics", which is funded by the Ministry of Education, Science and Technological Development.

References

[1] Wu, B., *et al.*, Optimal Power Management for a Hydraulic Hybrid Delivery Truck, *Vehicle System Dynamics*, *42* (2004), 1-2, pp. 23-40

[2] Tavares, F., *et al.*, Simulation study of advanced variable displacement engine coupled to power-split hydraulic hybrid powertrain, *Journal of Engineering for Gas Turbines and Power*, *133* (2011), 12, pp. 122803.

[3] Filipi, Z., Hydraulic and pneumatic hybrid powertrains for improved fuel economy in vehicles, in: *Alternative Fuels and Advanced Vehicle Technologies for Improved Environmental Performance* (Ed. R. Folkson), Woodhead Publishing, 2014, pp. 505-540

[4] Kitanović, M. N., *et al.*, Fuel Economy Comparative Analysis of Conventional and Ultracapacitors-Based, Parallel Hybrid Electric Powertrains for a Transit Bus, *Proceedings*, 5th International Congress Motor Vehicles & Motors, Kragujevac, Serbia, 2014, pp. 258-267

[5] Kitanović, M. N., *et al.*, Dynamic Programming Study of a Hybrid Electric Powertrain System for a Transit Bus, *Proceedings*, 18th Symposium on Thermal Science and Engineering of Serbia, Sokobanja, Serbia, 2017, pp. 988-997

[6] Guzzella L., Sciarretta, A., *Vehicle Propulsion Systems*, Springer, 2013

[7] Kitanović, M. N., *et al.*, A Simulation Study of Fuel Economy Improvement Potentials of a Transit Bus, *Proceedings*, 24th International Automotive Conference Science and Motor Vehicles, Belgrade, Serbia, 2013, pp. 56-67

[8] ***, Axial piston variable pump (A)A4VSO Data sheet, https://dc-us.resource.bosch.com/media/us/products_13/product_groups_1/industrial_hydraulics_5/pdfs_4/ra92050.pdf

[9] Pourmovahed, A., *et al*., Modeling of a Hydraulic Energy Regeneration System-Part I: Analytical Treatment, *Journal of Dynamic Systems, Measurement, and Control, 114* (1992), 1, pp. 155-159

[10] Pourmovahed, A., Energy Storage Capacity of Gas-Charged Hydraulic Accumulators, *Proceedings*, 23rd Thermophysics, Plasmadynamics and Lasers Conference, San Antonio, Texas, 1988, pp. 1-11

[11] Bellman, R. E., Dreyfus, S. E., *Applied Dynamic Programming*, Princeton University Press, 1962

[12] Kirk, D. E., *Optimal Control Theory: An Introduction*, Dover Publications, 2004

[13] Sundström, O., Guzzella, L., A generic dynamic programming Matlab function, *Proceedings* (2009 IEEE control applications (CCA) & intelligent control (ISIC)), 3rd IEEE multi-conference on systems and control, St. Petersburg, Russia, 2009, pp. 1625-1630

[14] McBride, B. J., *et al.*, NASA Glenn Coefficients for Calculating Thermodynamic Properties of Individual Species, Report No. E-13336, National Aeronautics and Space Administration, John H. Glenn Research Center at Lewis Field, Cleveland, Ohio, 2002